Author(s): Das, Sujoy; Rissanen, Kari; Sahoo, Prithidipa

Title: Rare Crystal Structure of Open Spirolactam Ring along with the Closed-Ring Form of a Rhodamine Derivative : Sensing of Cu2+ Ions from Spinach

Year: 2019

Version: Published version

Please cite the original version:

Das, S., Rissanen, K., & Sahoo, P. (2019). Rare Crystal Structure of Open Spirolactam Ring along with the Closed-Ring Form of a Rhodamine Derivative : Sensing of Cu2+ Ions from Spinach. ACS Omega, 4(3), 5270-5274. https://doi.org/10.1021/acsomega.9b00053

ACS OMEGA

Article

Cite This: ACS Omega 2019, 4, 5270−5274

http://pubs.acs.org/journal/acsodf

Rare Crystal Structure of Open Spirolactam Ring along with the Closed-Ring Form of a Rhodamine Derivative: Sensing of Cu^{2+} Ions from Spinach

Sujoy Das,[†] Kari Rissanen,[‡] and Prithidipa Sahoo*[,†]

[†]Department of Chemistry, Visva-Bharati University, Santiniketan 731235, West Bengal, India

[‡]Nanoscience Centre, Department of Chemistry, University of Jyvaskyla, Survontie 9B, P.O. Box 35, 40014 Jyväskylä, Finland

Supporting Information

ABSTRACT: Crystal structures of a rhodamine derivative in its closed and open spirolactam ring forms were developed, which allows selective and sensitive detection of Cu^{2+} ions at a micromolar range in neutral medium. The chemosensing properties of the probe through a pentacoordinate Cu^{2+} ions were proven by spectroscopic and theoretical analysis. The spirolactam ring opening as the Cu^{2+} selective sensor was applied to spinach (*Spinacia oleracea*) to estimate the accumulation of copper as copper(II) in the plant.

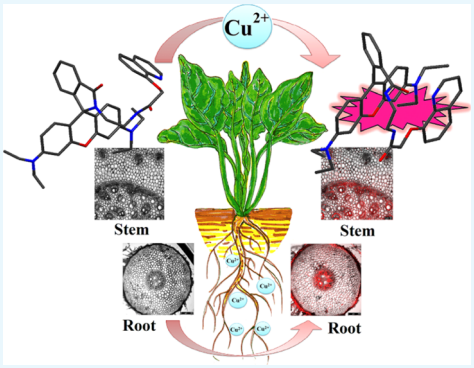

1. INTRODUCTION

Copper (Cu) holds the position of the third most abundant essential trace element just after iron and zinc.[1−4] Certain level of copper is crucial to the health of animals, ranging from bacteria to mammals, as well as the plant kingdom.[5] In the animal body system, copper's potent redox activities let it play the vital role in haemopoiesis and iron absorption and as a catalytic cofactor for various metalloenzymes, including Cu/Zn superoxide dismutase, cytochrome *c* oxidase, and tyrosinase.[6,7] According to the World Health Organization (1996), average copper requirements are 50 μg/kg and about 12.5 μg/kg of body weight per day for infants and adults, respectively.[8] Possession of abnormal level of copper in living body systems may consequent neurodegenerative diseases, including Alzheimer's disease, Wilson's disease, Menke's disease, liver or kidney damage, prion diseases, oxidative stress, familial amyotropic lateral sclerosis, and can boost up many other diseases, even cancer.[9−14] In living plant systems, the presence of copper is found to be in the range of 0.05−0.5 ppm for a growing medium, whereas in most tissues, the normal range is between 3 and 10 ppm.[15] Copper is essential in the process of photosynthesis, plant respiration, plant metabolism of carbohydrates and proteins, and in several enzyme systems including the enzymes which are involved in lignin synthesis.[16−18] This trace element can also intensify flavor and color in vegetables and flowers. The elevated level of copper in a growing plant medium produces reactive oxygen species, which has the power to reduce protective enzyme activity, photosynthesis, growth, to cause ion leakage in cell membranes, and can even lead to death of the medium.[19−24] Free Cu^{2+} are considered as the most toxic form of copper to organisms and to the environment. The malignant behavior of Cu^{2+} imposes a strong need for a reliable practical sensing method to selectively detect Cu^{2+} ions in the living system. Among the various analytical methods, fluorescence chemosensors attract much more attention because of their simplicity, selectivity, low-cost, and real-time sensing.[25−27] To fulfill the purpose of a fluorescence turn-on chemosensor, rhodamine dyes are widely used due to their excellent spectroscopic properties, such as long wavelength excitation and emission profiles, large extinction coefficients, high fluorescence quantum yields, and the intense pink coloration after spirolactam ring opening.[28−30] Thus far, the work done for Cu^{2+} sensing is mainly accomplished in live cell systems (comparison Table S1). We have now focused on plant tissues, which are one of the main sources of Cu^{2+} accumulation in animals.

2. RESULTS AND DISCUSSION

2.1. Plausible Mechanism. Inspired by previous studies, we propose a mechanism where our chemosensor **QRA** (quinoline rhodamine acetamide) in its closed form first coordinates with copper perchlorate to form a fluorescent intermediate pentacoordinate **QRA**−Cu^{2+} complex (see the Supporting Information computations), which upon hydration loses the copper ion to form the stable fluorescent **QRA** in the

Received: January 7, 2019
Accepted: March 1, 2019
Published: March 13, 2019

DOI: 10.1021/acsomega.9b00053
ACS Omega 2019, 4, 5270−5274

open form (Scheme 1). A strong $\pi-\pi$ stacking between the quinoline and xanthene moieties at a distance of ca. −3.4 Å

Scheme 1. Proposed Mechanism of Interaction between QRA and Cu^{2+} in Neutral Aqueous Medium

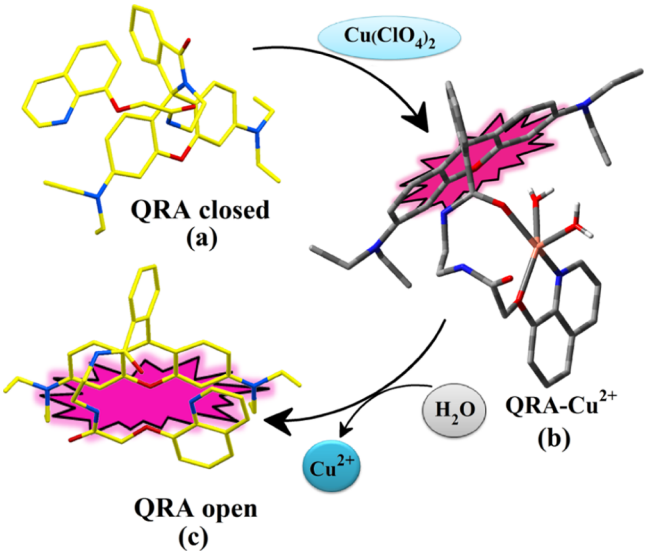

(see the following X-ray structures) counts for the exceptional stability of the open form of the **QRA**. We managed to get single crystals of moderate diffraction quality from both forms, **QRA-closed** and **QRA-open**, by diffusing petroleum ether into an acetonitrile solution of **QRA-closed/open** in a closed vessel.

2.2. Crystallographic Studies. The X-ray structure (Figure 1a) of the **QRA**-closed reveals the nonfluorescent edge-to-face orientation of the xanthene and quinoline moieties (Figure S4), where the center of the quinoline ring is 6.5 Å away from the center of the xanthene ring. The spirolactam ring opening in **QRA**-open manifests a huge conformational change. The quinoline ring moves ca. 2 Å, twists ca. 70°, and slides under the xanthene moiety, resulting in a very strong coplanar $\pi-\pi$ stacking interaction at 3.4 Å of the xanthene and quinoline rings (Figures 1b and S5).

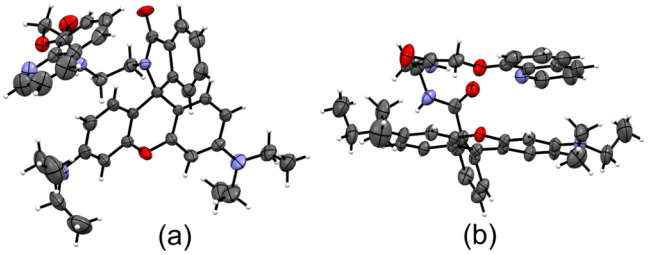

Figure 1. ORTEP plots of **QRA**-closed (a) and **QRA**-open (b), the perchlorate ions and lattice waters in **QRA-open** are omitted for clarity. The thermal ellipsoids are drawn at the 50% probability level.

2.3. Spectral Behavior of QRA. To demonstrate the interactions between the probe **QRA** and Cu^{2+} ions, absorbance and fluorescence titrations were carried out in CH_3CN-H_2O (1:8, v/v) at neutral pH (pH 7.2, 10 mM Tris-HCl buffer). A 10 μM solution of **QRA** was titrated against some known concentrations of Cu^{2+}, where the maximum absorbance and fluorescence were observed after addition of 30 μM of copper (3 equiv). The spectra shows a decreased absorbance at 312 nm followed by an increasing absorbance at 530 nm with a notable isosbestic point at 334 nm (Figure 2a), which is probably due to $\pi-\pi^*$ transition from the quinoline to xanthene moiety. Fluorimetric analysis curve upon excitation at 530 nm, showed a 130-fold hike in fluorescence at 574 nm (Figure 2b). The comparative spectrophotometric response of **QRA** was also studied in various biologically relevant cations (Figure S6) and different analytes (Figure S7), which confirmed the sensitivity (full fluorescence signal within 2 min) (Figure S8) and high selectivity of the probe toward Cu^{2+}, both in solution and solid phase (Figure S9). Binding interactions determine 1:1 stoichiometric ratio of **QRA** and Cu^{2+} in the Job's plot (Figure S10).[31] The probe **QRA** has a detection limit of 2.2 μM for Cu^{2+} ion (Figure S11).[32]

2.4. pH Titration. It is very important to maintain the pH of the medium while working with rhodamine derivatives. That is why we performed the pH titration of the probe **QRA** with Cu^{2+}. It clearly reflects the nondependence of **QRA** on the pH range of 7−8 for copper(II) detection (Figure S12).

2.5. NMR Spectroscopic Titration. ^1H NMR titration (CD_3CN) reveals that the aromatic protons of probe **QRA** shifted upfield abruptly and became broader upon addition of 1 equiv Cu^{2+}, which represents the increase in electron density of the xanthene ring (Figure S13). In ^{13}C NMR titration, the more significant spiro cycle carbon peak at 70.75 ppm is shifted to 131.09 ppm (Figure S14). These coordinations led to the changes from closed to an open spiro cycle in the absorption-emission spectra and a sharp electronic transition from quinoline to the xanthene moiety.

2.6. Theoretical Analysis. Potential energy surfaces of the three structures, that is, **QRA closed**, **QRA**−Cu^{2+}, and **QRA**

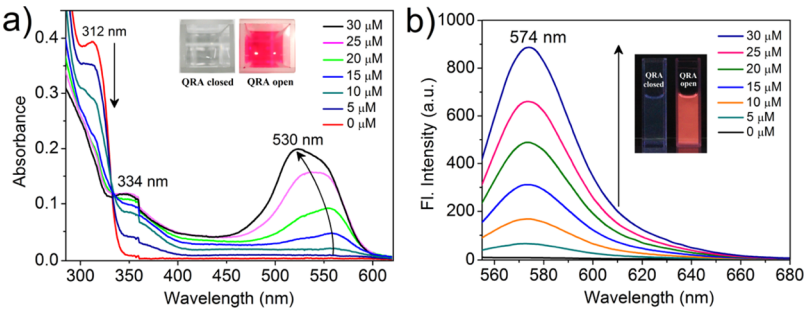

Figure 2. (a) UV−vis absorption spectra of **QRA** (10 μM) after addition of Cu^{2+} upto 3 equiv in CH_3CN/H_2O 1:8 (v/v), (pH 7.2, 10 mM Tris-HCl buffer). (b) Fluorescence emission spectra (λ_{ex} = 530 nm) of **QRA** (10 μM) after addition of Cu^{2+} upto 3 equiv (inset) visual and fluorescence changes after addition of Cu^{2+}.

DOI: 10.1021/acsomega.9b00053
ACS Omega 2019, 4, 5270−5274

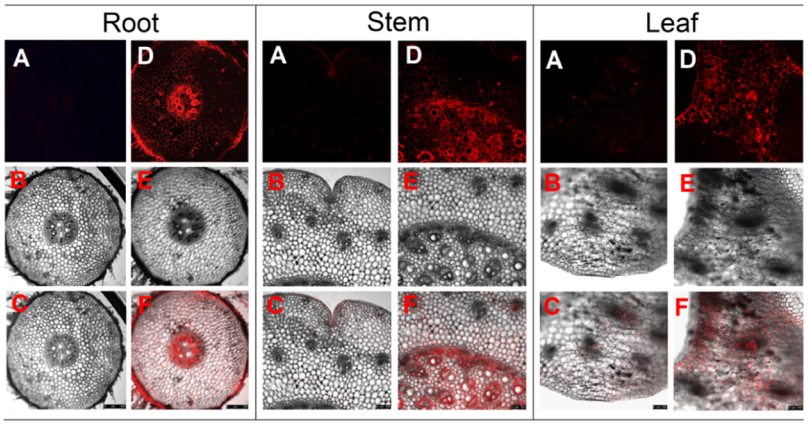

Figure 3. Confocal microscopic images of the root, stem, and leaf taken from spinach plant. (A,D) are the fluorescent images, (B,E) are the brightfield images, and (C,F) are the overlay images. Scale bars are in the range of 0−250 μm.

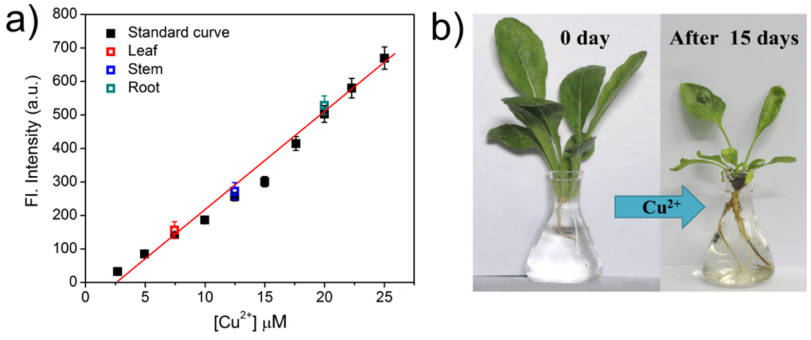

Figure 4. (a) Estimation of the concentration of copper(II) ion in different parts of the spinach plant with the help of a standard fluorescence curve. Standard deviations are represented by error bars (n = 3). (b) Photographic image of a spinach sapling (*S. oleracea*) treated with 10 mM Cu^{2+} solution followed by treatment with a 10 mM **QRA** solution in acetonitrile−water (1:10, v/v) for 15 days.

open were optimized using DFT at CAM-B3LYP level using the 6-31G**/LANL2DZ basis set and CPCM (water) solvent model.[33] From Figure S15, it has been shown that Cu^{2+} ions forms a pentacoordinated complex with **QRA** in its most-stabilized geometry with the N and O centers of **QRA** along with water molecules. The energy of **QRA** open was minimized by an amount of 37.65 kcal/mol from the initial closed structure of **QRA** (Table S2). The aforesaid spectroscopic and theoretical analysis corroborates with our proposed mechanism.

2.7. Imaging and Estimation. Accumulation of the copper(II) ion was instigated in Indian spinach (*Spinacia oleracea*, family: Amaranthaceae), the stem and leaf of which are a popular vegetable throughout the globe. A 7-days old sapling was taken for the study. Initially, it was kept in a neutral aqueous solution of 10 mM copper perchlorate for a week, followed by 10 mM aqueous solution of **QRA** for another week. Then, the transverse sections of three different parts, that is, root, stem, and leaf were done and collected separately in three Petri dishes, and each section was observed under a confocal microscope.

The images in Figure 3 represent that the copper(II) ion was mainly absorbed through the xylem tissue of the root showing the highest fluorescence signal, whereas the pith and endodermis region displayed negligible fluorescence. In the stem, intense fluorescence response from the vascular bundle and in the leaf and relatively lower fluorescence from the collenchyma cell region is observed. The exact concentration of accumulated Cu^{2+} ions in the sapling has been estimated with the help of standard fluorescence spectra, which measure 20, 12.6, and 7.8 μM of copper ion in root, stem, and leaf, respectively (Figure 4).

3. CONCLUSIONS

In conclusion, we can say that to the best of our knowledge this is the first report where we developed a rare crystal structure of rhodamine derivative (**QRA**) with an open spirolactam ring. **QRA** can selectively recognize Cu^{2+} in aqueous medium with very low concentration. The selective turn-on sensing of **QRA** toward Cu^{2+} was successfully demonstrated in a spinach sapling to estimate the concentration of copper(II) ions present in the root, stem, and leaf of that sapling. More interestingly, this unique chemosensing method can easily estimate Cu^{2+} without abstracting it from the tested sample.

4. EXPERIMENTAL DETAILS

4.1. Materials and Methods. Rhodamine B, ethylenediamine, bromoacetyl chloride, 8-hydroxyquinoline, copper(II) perchlorate, and other metal salts were purchased from Sigma-Aldrich Pvt. Ltd. (India). All other materials were obtained from local suppliers and used without further purification. Solvents were dried according to standard procedures. Crystal structures were diffracted in a Bruker Single Crystal X-ray diffractometer. ^{1}H and ^{13}C NMR spectra were recorded on a Bruker 400 MHz instrument. For NMR spectra and NMR titration, $CDCl_3$ and CD_3CN were used as solvents, using an internal standard of trimethylsilane. Chemical shifts are

DOI: 10.1021/acsomega.9b00053
ACS Omega 2019, 4, 5270−5274

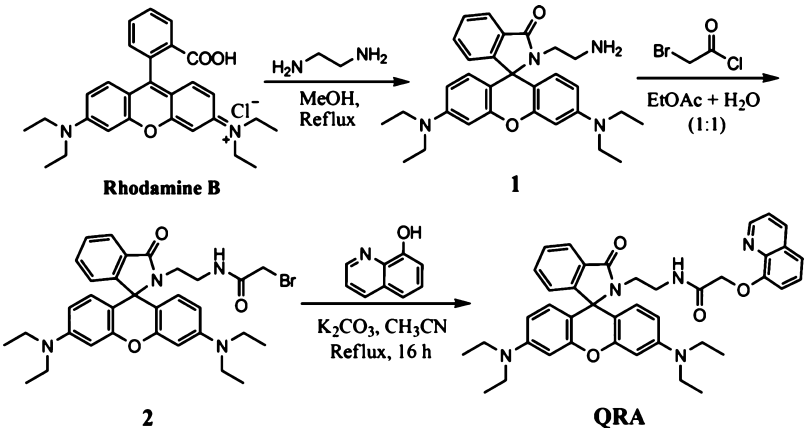

Figure 5. Synthesis of **QRA**.

expressed in δ ppm units. ^{1}H−^{1}H and ^{1}H−C coupling constants are denoted in Hz. High-resolution mass spectrometry (HRMS) was carried out using a micromass Q-TOF Micro instrument. Fluorescence and absorbance spectra were recorded on a PerkinElmer model LS55 and SHIMADZU UV-3101PC spectrophotometers, respectively. Elemental analysis was carried out on PerkinElmer 2400 series CHNS/O Analyzer. The following abbreviations are used to describe spin multiplicities in ^{1}H NMR spectra: s = singlet; d = doublet; t = triplet; m = multiplet.

For confocal microscopy, a Leica TCS SP8 laser scanning confocal microscope system was used. Images obtained through section scanning were analyzed by the LasX software with excitation at 530 nm monochromatic laser beam, and emission spectra were integrated over the range 574 nm (single channel) with 10× magnification.

4.2. Synthesis and Characterization of QRA. The probe **QRA** was synthesized by the reaction between 8-hydroxyquinoline and a 2-bromoacetamide substituent of rhodamine B (**2**) following a previously published report from our lab (detailed synthesis of compound **2** from rhodamine B has been described in the Supporting Information).[32] To a solution of anhydrous K_2CO_3 (0.57 g, 4 mmol) in dry acetone was added 8-hydroxyquinoline (0.3 g, 2 mmol). The mixture was stirred for 0.5 h, followed by addition of compound **2** (1.25 g, 2 mmol) to the solution and subsequent refluxing for 24 h (Figure 5). Then, the reaction mixture was poured into cold water. The solution was extracted with CH_2Cl_2 (3 × 50 mL), and the combined organic layer was washed with 5% aqueous HCl (50 mL), 10% aqueous Na_2CO_3 (50 mL), and finally with water and then was dried over anhydrous $MgSO_4$. After evaporating the solvents, the residue was column chromatographed on silica gel (60−120 mesh) with chloroform/ethyl acetate = 3:1 v/v as the eluent to give 1 g (78%) of **QRA** as a white powder. ^{1}H NMR ($CDCl_3$, 400 MHz): δ (ppm) 8.79 (d, J = 2.4 Hz, 1H), 8.10−8.12 (dd, J = 8 Hz, 1H), 7.81 (s, 1H), 7.68−7.70 (dd, J = 8 Hz, 1H), 7.36−7.42 (m, 5H), 7.08−7.10 (dd, J = 8 Hz, 1H), 6.99−7.01 (m, J = 4 Hz, 1H), 6.34 (d, J = 4 Hz, 2H), 6.26−6.28 (d, J = 8 Hz, 2H), 6.07−6.10 (m, J = 12 Hz, 2H), 4.70 (s, 2H), 3.25−3.34 (m, 10H), 3.07−3.10 (t, J = 12 Hz, 2H), and 1.11−1.14 (t, J = 12 Hz, 12H). ^{13}C NMR ($CDCl_3$, 400 MHz): δ (ppm) 168.95, 168.59, 154.12, 153.84, 153.26, 149.57, 148.89, 140.57, 136.08, 132.52, 130.77, 129.55, 128.68, 127.89, 126.88, 123.80, 122.92, 121.91, 121.37, 111.70, 108.19, 105.34, 97.83, 69.68, 64.92, 44.41, 39.35, 38.22, and 12.72. HRMS (ESI-MS): anal. calcd for $C_{41}H_{43}N_5O_4$, 669.80; found, 670.80 [M + H$^+$, 100%]; Anal. Calcd for $C_{41}H_{43}N_5O_4$: C, 73.52; H, 6.47; N, 10.46; O, 9.55. Found: C, 73.50; H, 6.44; N, 10.47; O, 9.56.

■ ASSOCIATED CONTENT

Supporting Information

The Supporting Information is available free of charge on the ACS Publications website at DOI: 10.1021/acsomega.9b00053.

Crystallographic data for the closed form of **QRA** (CIF)

Crystallographic data for the open form of **QRA** (CIF)

Performance comparison; synthesis details; additional spectroscopic data; ^{1}H NMR, ^{13}C NMR, and mass spectra of **QRA**; crystallographic data; supplementary fluorescence images; DFT calculation details; estimation of copper in spinach plant (PDF)

■ AUTHOR INFORMATION

Corresponding Author

*E-mail: prithidipa@hotmail.com (P.S.).

ORCID

Sujoy Das: 0000-0003-3921-0999

Kari Rissanen: 0000-0002-7282-8419

Prithidipa Sahoo: 0000-0001-8493-7068

Notes

The authors declare no competing financial interest.

■ ACKNOWLEDGMENTS

P.S. acknowledges UGC, India for awarding her the start-up grant [project file no. F.30-7/2014 (BSR)]. S.D. is sincerely thankful to CSIR, India for the senior research fellowship. S.D. also thanks Pulak Kumar Maity, Ballygunge Science College, University of Calcutta and Mohit Lal Kumar, Dept. of Botany, Visva-Bharati for their sincere help. Authors are grateful to confocal microscopy facility, Visva-Bharati University.

■ REFERENCES

(1) Sigel, H. *Metal Ions in Biological Systems*; Marcel Dekker: New York, 1981; Vol. *12*.

(2) Malvankar, P. L.; Shinde, V. M. Ion-pair extraction and determination of copper(II) and zinc(II) in environmental and pharmaceutical samples. *Analyst* **1991**, *116*, 1081−1084.

(3) Waggoner, D. J.; Bartnikas, T. B.; Gitlin, J. D. The role of copper in neurodegenerative disease. *Neurobiol. Dis.* **1999**, *6*, 221−230.

DOI: 10.1021/acsomega.9b00053
ACS Omega 2019, 4, 5270−5274

(4) Barceloux, D. G.; Barceloux, D. Copper. *J. Toxicol., Clin. Toxicol.* **1999**, *37*, 217−230.
(5) Lippard, S. J.; Berg, J. M. *Principles of Bioinorganic Chemistry*; University Science Books: Mill Valley, CA, 1994.
(6) Hamza, I.; Gitlin, J. D. Copper Chaperones for Cytochrome *c* Oxidase and Human Disease. *J. Bioenerg. Biomembr.* **2002**, *34*, 381−388.
(7) Lopez-Serrano, D.; Solano, F.; Sanchez-Amat, A. Involvement of a novel copper chaperone in tyrosinase activity and melanin synthesis in Marinomonas mediterranea. *Microbiology* **2007**, *153*, 2241−2249.
(8) WHO. Copper in Drinking-water. *Background Document for Development of WHO Guidelines for Drinking-Water Quality*; WHO/SDE/WSH/03.04/88, 2004.
(9) Barnham, K. J.; Masters, C. L.; Bush, A. I. Neurodegenerative diseases and oxidative stress. *Nat. Rev. Drug Discovery* **2004**, *3*, 205−214.
(10) Gaggelli, E.; Kozlowski, H.; Valensin, D.; Valensin, G. Copper Homeostasis and Neurodegenerative Disorders (Alzheimer's, Prion, and Parkinson's Diseases and Amyotrophic Lateral Sclerosis). *Chem. Rev.* **2006**, *106*, 1995−2044.
(11) Bull, P. C.; Thomas, G. R.; Rommens, J. M.; Forbes, J. R.; Cox, D. W. The Wilson disease gene is a putative copper transporting P-type ATPase similar to the Menkes gene. *Nat. Genet.* **1993**, *5*, 327−337.
(12) Crichton, R. R.; Dexter, D. T.; Ward, R. J. Metal based neurodegenerative diseases-From molecular mechanisms to therapeutic strategies. *Coord. Chem. Rev.* **2008**, *252*, 1189−1199.
(13) Hahn, S. H.; Tanner, M. S.; Danke, D. M.; Gahl, W. A. Normal Metallothionein Synthesis in Fibroblasts Obtained from Children with Indian Childhood Cirrhosis or Copper-Associated Childhood Cirrhosis. *Biochem. Mol. Med.* **1995**, *54*, 142−145.
(14) Hancock, C. N.; Stockwin, L. H.; Han, B.; Divelbiss, R. D.; Jun, J. H.; Malhotra, S. V.; Hollingshead, M. G.; Newton, D. L. A copper chelate of thiosemicarbazone NSC 689534 induces oxidative/ER stress and inhibits tumor growth in vitro and in vivo. *Free Radicals Biol. Med.* **2011**, *50*, 110−121.
(15) Bloodnick, E. *Fundamentals of Growing Media*; Promix, 2018.
(16) Sharma, S.; Sharma, S.; Upreti, N.; Sharma, K. P. Monitoring toxicity of an azo dye methyl red and a heavy metal Cu, using plant and animal bioassays. *Toxicol. Environ. Chem.* **2009**, *91*, 109−120.
(17) Mazhoudi, S.; Chaoui, A.; Habib Ghorbal, M.; El Ferjani, E. Response of antioxidant enzymes to excess copper in tomato (Lycopersicon esculentum, Mill.). *Plant Sci.* **1997**, *127*, 129−137.
(18) Lin, C.-C.; Chen, L.-M.; Liu, Z.-H. Rapid effect of copper on lignin biosynthesis in soybean roots. *Plant Sci.* **2005**, *168*, 855−861.
(19) Hötzer, B.; Ivanov, R.; Brumbarova, T.; Bauer, P.; Jung, G. Visualization of Cu^{2+} uptake and release in plant cells by fluorescence lifetime imaging microscopy. *FEBS J.* **2012**, *279*, 410−419.
(20) Pena, L. B.; Méndez, A. A. E.; Matayoshi, C. L.; Zawoznik, M. S.; Gallego, S. M. Early response of wheat seminal roots growing under copper excess. *Plant Physiol. Biochem.* **2015**, *87*, 115−123.
(21) Teisseire, H.; Guy, V. Copper-induced changes in antioxidant enzymes activities in fronds of duckweed (Lemna minor). *Plant Sci.* **2000**, *153*, 65−72.
(22) Halliwell, B.; Gutteridge, J. M. C. Oxygen toxicity, oxygen radicals, transition metals and disease. *J. Biochem.* **1984**, *219*, 1−14.
(23) Atha, D. H.; Wang, H.; Petersen, E. J.; Cleveland, D.; Holbrook, R. D.; Jaruga, P.; Dizdaroglu, M.; Xing, B.; Nelson, B. C. Copper Oxide Nanoparticle Mediated DNA Damage in Terrestrial Plant Models. *Environ. Sci. Technol.* **2012**, *46*, 1819−1827.
(24) Ruzsa, S. M.; Scandalios, J. G. Altered Cu Metabolism and Differential Transcription of Cu/ZnSodGenes in a Cu/ZnSOD-Deficient Mutant of Maize: Evidence for a Cu-Responsive Transcription Factor. *Biochemistry* **2003**, *42*, 1508−1516.
(25) Ghosh, A.; Das, S.; Sarkar, H. S.; Kundu, S.; Sahoo, P. Consumption of H_2S from Our Daily Diet: Determination by a Simple Chemosensing Method. *ACS Omega* **2018**, *3*, 11617−11623.
(26) Sarkar, H. S.; Das, S.; Uddin, M. R.; Mandal, S.; Sahoo, P. Selective Recognition and Quantification of 2,3-Bisphosphoglycerate in Human Blood Samples by a Rhodamine Derivative. *Asian J. Org. Chem.* **2017**, *6*, 71−75.
(27) Sahoo, P.; Sarkar, H. S.; Das, S.; Maiti, K.; Uddin, M. R.; Mandal, S. Pyrene appended thymine derivative for selective turn-on fluorescence sensing of uric acid in live cells. *RSC Adv.* **2016**, *6*, 66774−66778.
(28) de Silva, A. P.; Gunaratne, H. Q. N.; Gunnlaugsson, T.; Huxley, A. J. M.; McCoy, C. P.; Rademacher, J. T.; Rice, T. E. Signaling Recognition Events with Fluorescent Sensors and Switches. *Chem. Rev.* **1997**, *97*, 1515−1566.
(29) Callan, J. F.; de Silva, A. P.; Magri, D. C. Luminescent sensors and switches in the early 21st century. *Tetrahedron* **2005**, *61*, 8551−8588.
(30) Kim, J. S.; Quang, D. T. Calixarene-Derived Fluorescent Probes. *Chem. Rev.* **2007**, *107*, 3780−3799.
(31) Yu, C.; Zhang, J.; Li, J.; Liu, P.; Wei, P.; Chen, L. Fluorescent probe for copper(II) ion based on a rhodamine spirolactame derivative, and its application to fluorescent imaging in living cells. *Microchim. Acta* **2011**, *174*, 247−255.
(32) Das, S.; Sarkar, H. S.; Uddin, M. R.; Mandal, S.; Sahoo, P. A chemosensor to recognize N-acyl homoserine lactone in bacterial biofilm. *Sens. Actuators, B* **2018**, *259*, 332−338.
(33) Frisch, M. J.; Trucks, G. W.; Schlegel, H. B.; Scuseria, G. E.; Robb, M. A.; Cheeseman, J. R.; Scalmani, G.; Barone, V.; Mennucci, B.; Petersson, G. A.; Nakatsuji, H.; Caricato, M.; Li, X.; Hratchian, H. P.; Izmaylov, A. F.; Bloino, J.; Zheng, G.; Sonnenberg, J. L.; Hada, M.; Ehara, M.; Toyota, K.; Fukuda, R.; Hasegawa, J.; Ishida, M.; Nakajima, T.; Honda, Y.; Kitao, O.; Nakai, H.; Vreven, T.; Montgomery, J. A., Jr.; Peralta, J. E.; Ogliaro, F.; Bearpark, M.; Heyd, J. J.; Brothers, E.; Kudin, K. N.; Staroverov, V. N.; Kobayashi, R.; Normand, J.; Raghavachari, K.; Rendell, A.; Burant, J. C.; Iyengar, S. S.; Tomasi, J.; Cossi, M.; Rega, N.; Millam, J. M.; Klene, M.; Knox, J. E.; Cross, J. B.; Bakken, V.; Adamo, C.; Jaramillo, J.; Gomperts, R.; Stratmann, R. E.; Yazyev, O.; Austin, A. J.; Cammi, R.; Pomelli, C.; Ochterski, J. W.; Martin, R. L.; Morokuma, K.; Zakrzewski, V. G.; Voth, G. A.; Salvador, P.; Dannenberg, J. J.; Dapprich, S.; Daniels, A. D.; Farkas, O.; Foresman, J. B.; Ortiz, J. V.; Cioslowski, J.; Fox, D. J. *Gaussian 09*, Revision A. 02; Gaussian, Inc.: Wallingford CT, 2009.

DOI: 10.1021/acsomega.9b00053
ACS Omega 2019, 4, 5270−5274